Front. Mater. Sci.
https://doi.org/10.1007/s11706-021-0567-3

REVIEW ARTICLE

Nanodiamonds as nanomaterial for biomedical field

Sarah GARIFO[1], Dimitri STANICKI[1], Gamze AYATA[1], Robert N. MULLER[1,2], and Sophie LAURENT (✉)[1,2]

1 General, Organic and Biomedical Chemistry Unit, Nuclear Magnetic Resonance (NMR) and Molecular Imaging Laboratory, University of Mons (UMONS), Avenue Maistriau 19, 7000 Mons, Belgium
2 Center for Microscopy and Molecular Imaging (CMMI), Rue Adrienne Bolland 8, 6041 Gosselies, Belgium

ABSTRACT: Recent advances in nanotechnology have attracted significant attention to nanodiamonds (NDs) in both industrial and research areas thanks to their remarkable intrinsic properties: large specific area, poor cytotoxicity, chemical resistance, magnetic and optical properties, ease of large-scale production, and surface reactivity make them suitable for numerous applications, including electronics, optics, sensors, polishing materials, and more recently, biological purposes. Growing interest in diamond platforms for bioimaging and chemotherapy is observed. Given the outstanding features of these particles and their ease of tuning, current and future applications in medicine have the potential to display innovative imaging applications and to be used as tools for monitoring and tracking drug delivery *in vivo*.

KEYWORDS: nanodiamond; scale-up synthesis; bioimaging; hyperpolarization; drug delivery

Contents

Received May 9, 2021; accepted August 1, 2021

E-mail: sophie.laurent@umons.ac.be

1 Introduction

Over the past decades, nanosciences have attracted scientific and technological attention due to the unique structure and remarkable properties of nanometric objects [1–3]. Among them, carbon nanomaterials (CNMs) have garnered significant interest for numerous technical applications in various fields, including electronics [4–5], composites, sensors and medical applications. The enormous diversity of CNMs results from their ability to form

different hybridized orbitals and bonds that complement the well-known forms of the structured carbon family (i.e., diamond, graphite, graphene, fullerene, and nanotube). More recently, nanoscale diamond particles, also known simply as nanodiamonds (NDs), have emerged as a relatively new class of CNMs that has gained consideration over the years as alternative carbon-based materials. From a structural point of view, NDs will present different features depending on their preparation method. In that respect, if detonation obtained NDs (i.e., DET NDs) are represented by a complex structure including a diamond core with defects, a transient nondiamond layer and an outer shell exhibiting various functional groups (diamond cores are covered by other allotropic carbon forms, such as graphite and/or noncarbon impurities surrounding the sp^3-hybridized core, due to treatment conditions), high temperature/pressure obtained NDs (i.e., HPHT NDs) are highly crystalline structure. Their morphology has a nearly spherical shape (i.e., DET NDs), irregular or faceted (i.e., HPHT, milled NDs) and their size can range from 1 to 200 nm [6–7]. NDs are classified into three groups according to their size [8]: diamond nanocrystals (10–150 nm), ultra-nanocrystalline diamond particles (2–10 nm) and diamondoids (1–2 nm). A high atomic density is obtained through strong covalent bonds between atoms in the diamond crystallographic lattice, which provides hardness and chemical inertness features and stability in a wide range of environments [9].

Depending on the synthesis procedure, core defects and impurities can be observed, resulting in interesting magnetic and optical properties. As an example, photoluminescence using NDs resulting from nitrogen vacancy defects exhibit stable photoemission properties (spectral range: 500–800 nm) [10] which could be useful for bioimaging applications. These unique features (i.e., hardness, biochemical inertness, magneto-optical properties, etc.) have created opportunities for many applications, such as catalysis [11], polymer strengthening, polishing, antibacterial and antifungal coating materials and even nanomedicine [12], for which recent reports highlighted the use of such particles in tissue engineering [13–14], coating (implantable) materials, gene therapy [15], protein mimics [16], diagnostic applications [17] and drug delivery [18]. Indeed, similar to other nanoscale particles, the large surface area enables conjugation of a high number of (bio)-molecules for intra- or extracellular delivery applications, which is particularly useful for chemotherapy. Moreover, NDs have emerged as promising materials for imaging applications such as magnetic resonance imaging (MRI), luminescence imaging or theranostic purposes through the grafting of various molecules (e.g., conventional contrast agents, biological vectors, and drugs). Many investigations exploiting their endogenous magnetic and fluorescent properties have led to the development of a new generation of imaging probes exclusively using NDs. Beyond these purposes, ND platforms have been explored as effective carriers for therapeutics and drug delivery since their surfaces provide versatile functional groups.

This short review aims to cover the properties and applications of NDs for the biomedical field (i.e., diagnosis and drug delivery). From synthesis techniques, intrinsic properties, platform design and biomedical applications, this review will summarize the promising interest that nanoscale diamond particles have generated to date, and some current challenges for future applications will be discussed.

2 Synthesis and physicochemical properties of NDs

Crucial parameters, such as size, shape, intrinsic properties and surface functions, are determined by the technique used for their production [5,19]. While some natural NDs have been found in meteorites, as evidenced by X-ray diffraction (XRD) data [20], a variety of synthetic processes affording ND particles, either through a top-down (i.e., the controlled fragmentations of micron-sized diamond) or a bottom-up approach (i.e., building the carbon lattice from carbon molecular precursors), have been reported [21]. Among other techniques, we can reference the use of ultrasound cavitation [22], plasma-assisted chemical vapor deposition (CVD) [23] or CVD milled boron-doped procedure [4], laser ablation [24], crushing and milling of larger high static pressure and high-temperature (HPHT) diamond microcrystals and dynamic techniques for the production of such particles. The laboratory-scale production method uses adamantane ($C_{10}H_{16}$), a monomolecular unit of diamond (diamondoid), which can reproduce the nano/microstructure of diamonds under HPHT conditions (8 GPa and temperature above 1300 °C [25]). In addition, the laser-assisted technique produces high-purity 4–5 nm particles using a much more expensive methodology than casual detonation and static synthesis, and the high cost does not allow for large-scale production [5].

The most commonly used method is to detonate carbon-containing explosives (detonation technique, DET) uses an oxygen-deficient environment to avoid oxidation of the carbon [24]. The internal combustion requires an explosive mixture of trinitrotoluene (TNT; $C_6H_5N_3O_6$, 2-methyl-1,3,5-trinitrobenzene) and hexogen (RDX; $C_6H_6N_6O_6$, 1,3,5-trinitroperhydro-1,3,5-triazine) in a charge proportion of 60/40 (TNT/RDX) to increase ND yield from the detonation product [26]. The decomposition reaction is shown as follows [24]:

$$6\mathrm{CNOH} \rightarrow 3\mathrm{N_2} + 3\mathrm{H_2O} + \mathrm{CO} + \mathrm{CO_2} + 4\mathrm{C} \quad (1)$$

In the traditional synthesis, the detonation process takes place in a closed metallic chamber under an atmosphere of gas (e.g., N_2 and CO_2) or water (in the physical state of ice) whether the process occurs under dry or wet conditions, respectively. The drastic conditions created during the detonation process last a fraction of microseconds. During this time, NDs grow to a few nanometers in the form of nanodroplets and then transform into NDs after rapid cooling [25]. The charge-dependance has been studied according to the different physicochemical parameters of the resulted NDs. It was established that single digits increased in size (4–6 nm) while increasing the charge weight more than 17-fold during the detonation procedure [26].

Another technique has been developed by crashing microsized monocrystalline diamonds produced by non-dynamic processes, such as the HPHT method. HPHT NDs can be obtained from graphite or other carbon sources through these conditions, leading to the thermodynamic transition of the carbon phase from sp^2 to sp^3 hybridization. This process is quite versatile since the conditions of pressure and temperature are tuned to control the size of the resulted particles. Size discrimination undergoes a fragmentation process through a bead-assisted sonic disintegration or through a mechanical bead milling, providing high quality 20 nm up to a few microns NDs. This procedure is a well-described and reproducible top-down method [24].

Both synthetic approaches (i.e., detonation or HPHT) allow the large-scale production of NDs [24]. It should be highlighted that the resulting raw product is a mixture of NDs and ND clusters entrapped and coated with other carbon allotropes (25–85 wt.%) and noncombustible impurities (metals, oxides and salts; 1–8 wt.%) introduced by the detonation itself and by the chamber [27–28] (e.g., the steel walls of the blast chamber, the charge suspension device, the copper or lead igniter) in the case of detonation production or by the grinding process (i.e., HPHT). The process to isolate the diamond crystals from the mixture (30–75 wt.% of the diamond phase) involves oxidizing agents (e.g., H_2SO_4/HNO_3, $KMnO_4$, O_3/catalyst), mineral acid treatment (e.g., HCl, HNO_3, $HClO_4$) [28] and a deagglomeration procedure with milling samples using micrometer-sized zirconium oxide beads [5]. More recently, salt and sugar-assisted milling [29], or thermal and chemical treatment [24] have also been proposed. However, some functional groups are introduced as a result of the purification steps. DET NDs that result from the detonation procedure have homogeneous average size particles with a very narrow size distribution of 4–5 nm for a single digit with an oval shape (Fig. 1(a)), while statically HPHT NDs display an irregular sharp shape of 10–20 nm, as evidenced by transmission electron microscopy (TEM) image in Fig. 1(c). HPHT NDs also show a lower tendency to form agglomerates in comparison with DET NDs due to their different surface potentials (resulting from the wide variety of functional groups exhibited by DET NDs), as shown in TEM and scanning electron microscopy (SEM) images in Fig. 1 [30–31].

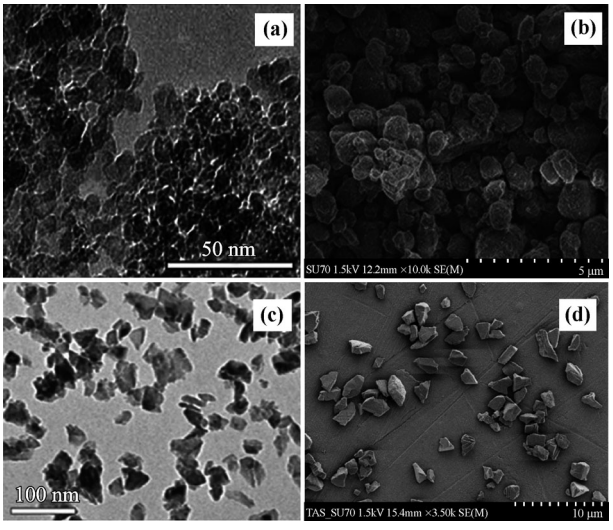

Fig. 1 Morphology and size distribution of NDs from dynamic and static synthesis observed with TEM (left column) and SEM (right column) of **(a)(b)** single digit DET NDs [30] and **(c)(d)** HPHT NDs [30–31]. Reproduced with permission from Refs. [30–31].

Overall, processes such as HPHT and DET have shown a high degree of potential and versatility to produce a wide variety of NDs from their structure to their intrinsic properties [32]. HPHT-synthesized NDs could be obtained

with different sizes ranging from a few nanometers to micrometers with monocrystalline structures [33]. In addition, HPHT NDs have a lower amount of sp^2 carbon than DET NDs remaining after purification and generally, present a higher degree of polydispersity than DET NDs. HPHT particles are particularly suitable for biological applications using their nitrogen-vacancy fluorescent properties as a result of a higher crystallinity. Additionally, color centers are more easily generated in top-down HPHT fragmentations of micron-sized diamond method than in detonation procedure because HPHT NDs can host more defects (minimum 5-fold larger HPHT NDs than DET NDs). It has been demonstrated that the nitrogen content in DET NDs can be controlled through an adequate selection of the precursor materials [26].

Overall, HPHT and DET NDs show various interests for a wide variety of applications in medicine. However, the appropriate characteristics must be taken into consideration when using these particles (e.g., intrinsic properties). In addition, surface modifications are usually performed to improve ND properties.

3 Preparation of ND platforms for biomedical applications

Diamond is generally considered a stable, chemically inert and biocompatible carbon material [34]. An isolated particle (e.g., DET ND) contains the following constituents [5]:

• A spherical core of sp^3-hybridized carbon atoms consisting of a typical diamond tetrahedral crystal lattice of approximately 4.5 nm containing 70%–90% of the carbon diamond-like structure of the particle weight according to X-ray data.

• An inhomogeneous outer layer composed of amorphous sp^2 carbon atoms, which contains various defects and heteroatoms (e.g., from the detonation synthesis: Fe, Cr, Ni, Al, Si, Ca) [35] giving the dark gray appearance of the colloidal suspension.

• A multifunctional surface layer containing heteroatoms such as ^{12}C, ^{14}N, and ^{16}O that results in a variety of functional groups on the surface. These compounds are involved in hydroxylic, carboxylic, ketonic, lactonic, ether, ester, anhydride and other groups from synthesis and purification treatments due to oxidation.

This last point is certainly a key feature that provides a high degree of flexibility. A number of interesting functionalization schemes has been developed to tailor surface modifications for (non)covalent attachment. These are summarized in Fig. 2 [28,36–39], where a wide variety of groups are explored for suitable potential applications involving *in vitro* and *in vivo* targeted delivery and bioimaging [36–38,40–57].

Strategies include carboxyl surface terminations for bioapplications and attachment of contrast agents, polymeric chains, peptides and/or nucleic acids bearing primary amine functions, while others involve immobilization of (bio)molecules, drugs or composites.

3.1 Surface oxidation

At the end of a typical synthesis and after the purification steps, the surface of the NDs is covered with oxygen-rich carbon functional groups from purification by sp^2 carbon oxidation conditions (e.g., as aldehydes, ketones), and many of them can be oxidized into carboxylic acid functional groups. Further oxidation treatment increases the content of oxygen atoms, resulting in a more uniform outer surface in terms of functional groups due to the increased amount of carboxylic acid functional groups, leading to optimal coupling [58–60]. In this context, oxidative surface chemistry is generally performed (e.g., oxidizing acids, ozone [42], thermal [59,61]) and optimized to lead to a high degree of carboxylation. Air annealing is a particularly effective oxidation process. In this context, powders are thermally treated in a high-temperature furnace under ambient and static air (temperature range: 400–500 °C) [59,61–62]. The temperature at which oxidative etching begins on the surface is approximated by an oxygen optimization procedure by studying the results of thermogravimetric analysis (TGA), X-ray photoelectron spectroscopy (XPS) results and weight loss versus annealing time. The evolution of surface modifications is assessed using Fourier transmission infrared spectroscopy (FTIR), XPS and zeta potential analysis [59–61]. Following air annealing, the intensity of the carbonyl band in the FTIR spectra (1600 cm^{-1}) increases (Fig. 3(a)). The C – H vibrational peak (2920 cm^{-1}) is significantly reduced. XPS data have revealed that under efficient heat conditions, the graphitic carbon content decreases (Fig. 3(b)), while oxygen-containing species increase by a factor of 2 after air oxidation, especially in ether- and carbonyl-bonded carbons. Furthermore, these values indicate that the oxygen-containing surface functional groups are located on the ND surface at a higher concentration. After redispersion in aqueous suspension, the effect of pH on the ζ-potential is compared to untreated

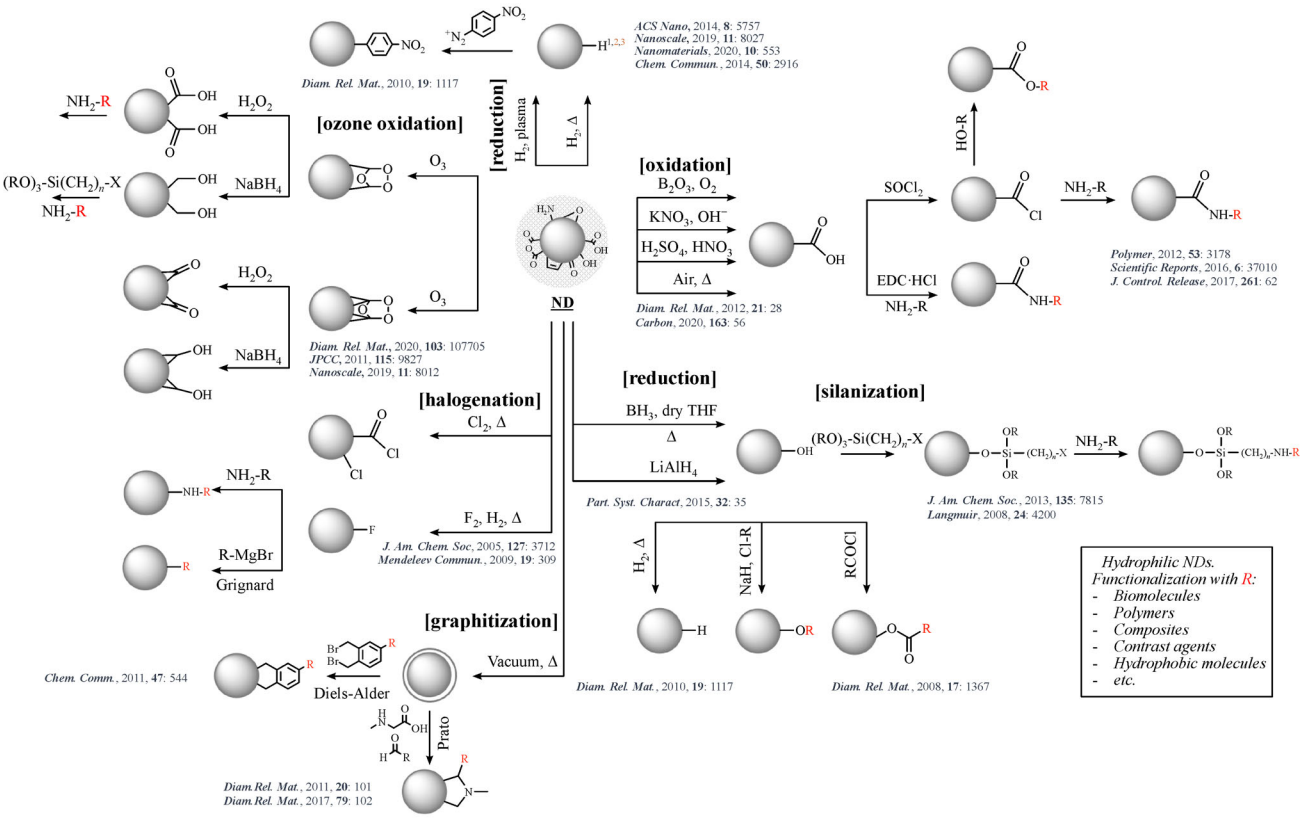

Fig. 2 Schemes to tailor surface modifications: surface homogenization, functional activation and covalent functionalization of NDs (ozone oxidation [40–42]; oxidation [43]; reduction [44–45]; functionalization [36–38,46]; silanization [47–48]; graphitization [49–51]; hydrogen microwave plasma and functionalization by diazonium coupling [52]; hydrogen isotopes (deuterium (H^2) and tritium (H^3)) incorporation for surface study [53–54] or labeling [55]; and halogenation [56–57]).

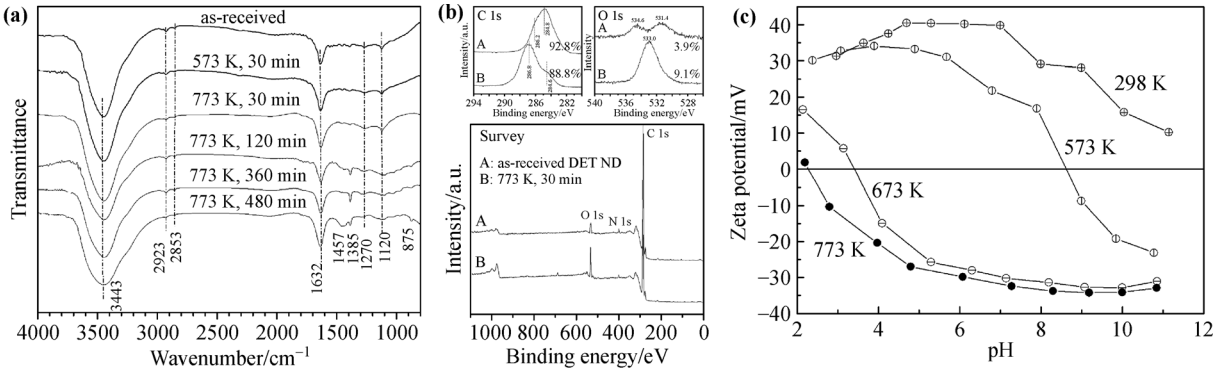

Fig. 3 Conversion into carboxylated DET NDs: **(a)** FTIR spectra; **(b)** XPS survey patterns and insets of C 1s and O 1s with their respective atomic percentage (A) before and (B) after air annealing at 773 K for 30 min; **(c)** Zeta potential versus pH. Reproduced with permission from Ref. [59] (Copyright American Chemical Society).

DET NDs and oxidized DET NDs (Fig. 3(c)) to investigate the electrostatic interactions in the suspensions. In the particular case of thermally treated powder, a strongly negative ζ-potential above pH 3 is obtained due to deprotonation of ND–COOH to ND–COO^- [28]. These experimental data are in good agreement with efficient surface modification.

3.2 Noncovalent coating strategies

Noncovalent functionalization is achieved through physical and chemical adsorption of specific small (bio)-molecules. This method has been reported as efficient to ensure stabilization of the suspension (i.e., interaction with polymers), prepare stable composites (i.e., polymers) or

serve as a complex for drug delivery (i.e., proteins, lipids, and drugs) [63].

3.3 Covalent coating strategies

Covalent surface strategies require the modification of surface functional groups. Some pathways performed on NDs include Diels–Alder reactions, Prato reactions, EDC chemistry, hydrogen isotopes incorporation, etc. Other strategies, including those involving inorganic materials such as silica layers on the NDs, are less common. Silica grafting involves the growth of inorganic silica shells or multilayers around hydroxylated NDs via *in situ* polymerization of a silica precursor (tetraethoxysilane (TEOS)) from the ND core directly [31] or from an emulsion via a liposome-based encapsulation process [48]. The use of functionalized silanes (i.e., (carboxyethyl) triethoxysilane (CETS), (3-aminopropyl) triethoxysilane (APTES)) allows for additional vectorized (bio)grafting (i.e., peptides, antibodies, nucleic acids) while providing high colloidal stability over wide pH ranges. Thus, the author of that study reported a facile surface modification process using silane chemistry and direct functionalization that can be explored in the biological field.

Because the surface is covered by a significant amount of carboxylic acid, a common approach relies on amine/carboxyl coupling to attach moieties. For example, polymer grafting provides stabilization. Hydrophilic polymers such as polyethylene glycol (PEG) or polyglycerol (PG) are widely used in nanotechnology to cover many materials due to their physicochemical and biological properties, including water solubility and biocompatibility [64]. Covalent conjugation of PEG chains on the nanoparticle surface can be achieved directly on ND–COOH systems via the EDC/NHS coupling process. For example, Terada et al. reported a one-pot preparation of hyperbranched polyglycerol NDs (HPHT ND–HPG–COOH) using this strategy that allowed for better dispersion in various environments. In addition, reactive sites were available for further grafting of compounds of interest bearing primary amine functions [65].

4 NDs in the biomedical field

NDs offer a unique combination of biologically and chemically relevant properties that make them advantageous alternatives to other nanoparticles. Because they are mostly composed of sp^3-hybridized carbons, it has been suggested that NDs are the hardest and the most biologically stable carbon allotrope. Many studies using cell viability tests of mitochondrial function (MTT) and luminescent ATP production assays have demonstrated that NDs are nontoxic to a variety of cell types [34,66–67]. *In vitro* genotoxicity studies (i.e., (oxidative) DNA or chromosomal damages mediated by oxidative stress) have shown significant differences according to the materials under investigation which differed from physiological properties (e.g., size, surface chemistry). Indeed, DET NDs (2–5 nm) were susceptible to induce cytotoxicity at higher concentrations, while genetic toxicity was observed to be stimulated at lower concentrations ($< 50\ \mu g \cdot mL^{-1}$) [68]. Besides, carboxylated HPHT NDs (20–100 nm) were reported to evidence any genotoxic activity ($100\ \mu g \cdot mL^{-1}$) [69] which attested their interest in bio-nanotechnology.

Overall, their promising applications in biomedicine include biosensing, coating for implantable materials, labeling for imaging modalities, tissue engineering, and drug and gene delivery. A brief overview of recent reports referring to the use of NDs for biomedical applications is given in Table 1 [7,37,64,70–88].

A key question regarding the non-biodegradable behavior of such NDs is related to the possible tissue accumulation and elimination pathway. To figure out, the short- and long-term distribution patterns in animals were investigated using labeled NDs (e.g., ^{125}I and ^{99m}Tc, ^{3}H or fluorescein dyes) or ND intrinsic defects (e.g., paramagnetic centers). In a recent study, Claveau et al. explored labeled ^{3}H-DET NDs produced by the radioactive analog tritium gas to monitor the distribution [55]. They observed that ^{3}H-DET NDs were accumulated mainly in the liver, lung, spleen and kidney after administration. In addition, in accordance with previous studies, small NDs (i.e., smaller than 10 nm) of size compatible with kidney elimination have been reported to be captured by liver cells, filtered by the glomerular system to be then eliminated while larger NDs (i.e., 50 nm) accumulate in tissues for few weeks after injection [55,89]. In another study, Purtov and coworkers showed the influence of the DET particle size (D_h: 150 and 300 nm) on the biodistribution in mice [89]. Their observations suggest that the size dependence is not significant. However, they found that unlike the smaller DET ND, the largest DET particles had accumulated in the liver after several days. Based on *ex vivo* EPR spectroscopy, intravenous administration of NDs (D_h: 70 nm; 40 mg per 1 kg body weight) into the tail veins of mice (26–28 g) has shown that most of the particles were removed from the bloodstream and trapped in the liver and spleen (2.5 h post-injection) [90].

Table 1 Some examples of modified NDs for biological purposes [7,37,64,70–88]

System	ND surface modification	Purposes	Outcomes	Refs.
ND-ODA/PLLA	ODA-functionalized NDs + PLLA	Bone tissue engineering [a)]	Good biocompatibility, increase in hardness, promising for bone scaffolds and smart surgical tools	[70]
ND·ANG-1 inside β-TCP	β-TCP scaffolds were modified with NDs functionalized with ANG-1	Bone implants [a)]	Improvement of vascularization and bone regeneration, safe and easy tool using NDs for biomolecule immobilization and delivery	[71]
ND-PEG·anti-HER2 peptide	Acid-treated NDs coupled with PEG and then conjugated to anti-HER2 peptide	CA for PAM [b)]	NDs accumulation in breast tumors, nontoxic particles	[72]
ND-Gd^{3+}(DO3A), ND-Mn^{2+}(EDTA)	Carboxylated ND surface conjugated to conventional amino Gd^{3+}/Mn^{2+} ion chelate	T_1-weighted MRI CA (1st generation) [b)]	T_1 contrast on MRI at high magnetic field	[73–74]
ND-PG-Gd^{3+}-DTPA	Carboxylated ND surface conjugated to functionalized Gd(III) chelate PG	T_1-weighted MRI CA (2nd generation) [b)]	Good dispersibility and high relaxometric properties	[75]
ND (HPHT, DET, natural)	Untreated or thermally oxidized	ND enhanced MRI via *in situ* hyperpolarization using OMRI, ^{1}H and ^{13}C MRI [b)]	No long-term toxicity of Gd(III), afford a different perspective to monitor and track functionalized ND *in vivo*	[76–79]
FND (HPHT NDs)	Intrinsic properties	Fluorescence imaging [b)]	High photostability (without photoblinking and photobleaching)	[80]
ND-dye	Covalently grafted dyes via click chemistry	Luminescence labeling [b)]	Fluorescent labeling that may undergo photobleaching	[81]
NDs·dBSA-PEG3000-biotin	Biopolymer-based coating	Stable fluorescent labeling for bioimaging [b)]	Stabilizing electrostatic and hydrophobic interactions to stabilize the systems	[82]
ND-OH·DOX (drug delivery)	Hydroxylated ND surface + drug (DOX) adsorbed (1st generation)	Increased uptake by breast and liver cancer cells [c)]	Tumor-growth inhibition	[83]
ND-PEG·DOX	Coating with PEG + DOX adsorbed (2nd generation)	Increased uptake, stabilization [c)]	Prevention of proteins and immune response adhesion, prolonged circulation time, tumor retention and better dispersion under physiological environment	[37,64,84]
ND-PAC	Covalent linkage of NDs to PAC	Drug delivery and cancer therapy [c)]	Decrease of ND-PAC complex cell viability of human lung (A549)	[85]
ND-PEG-FA·DOX	PEGylated NDs conjugated with folate and DOX	Increase in the specificity of drugs [c)]	Decrease of potential side effects, loading high number of DOX	[86]
ND-TAT-DOX	DOX and cell penetrating peptide (TAT) conjugated to the surface of oxidized NDs	Targeted drug release [c)]	To avoid premature release, optimization of intracellular drug delivery by enhancing the translocation across the cell membrane	[87]
ND·DOX, ND·EPI, ND·BLEO, ND·PAC, ND·MTX	Absorption of small hydrophobic anticancer drugs	Increased uptake [c)]	Improvement of drug retention	[7]
ND·PEI800·DNA (gene delivery)	Acid-treated ND surface coated with PEI + DNA	Gene therapy mediated by NDs [c)]	Higher transfection efficiency, enhancement of plasmid DNA delivery	[88]

a) Purpose on the aspect of tissue scaffolds. b) Purpose on the aspect of labeling. c) Purpose on the aspect of delivery agents.
Notes: "·" refers to the noncovalent interaction; "-" refers to the covalent bonding; β-TCP, β-tricalcium phosphate; ANG-1, Angiopoietin-1; BLEO, bleomycin; CA, contrast agent; dBSA, dodecyl benzenesulfonic acid; DET, detonation; DO3A, a gadoteridol macrocycle; DOX, doxorubicin; DTPA, diethylenetriaminepentaacetic acid; EDTA, ethylenediamine tetraacetic acid; EPI, epirubicin; FA, folic acid; FND, fluorescent nanodiamond; HPHT, high pressure high temperature; MRI, magnetic resonance imaging; MTX, mitoxantrone; ND, nanodiamond; ODA, octadecylamine; OMRI, Overhauser-enhanced magnetic resonance imaging; PAC, paclitaxel; PAM, photoacoustic microscopy; PEG, poly(ethylene glycol); PEI, polyethyleneimine; PG, polyglycerol; PLLA, poly(L-lactic acid); TAT, trans-activator of transcription protein.

4.1 NDs as tissue scaffolds and surgical implants

Tissue engineering is a new approach to repair or replace diseased tissues using biomaterials. These systems open many routes for their potential use as components of smart surgical tools, implants or bone scaffolds [91]. NDs show appropriate properties (i.e., strength, support adhesion, roughness, thermal stability) for tissue engineering [92]. Such agents were synthesized by Grausova et al. using NDs as a matrix on osteoblast-like MG 63 cells [14]. NDs provided good support for the adhesion and growth of cells in cultures. The study showed promising results using NDs in tissue engineering, particularly for their applications as implantable surface bone materials. Eivazzadeh-Keihan et al. reported that various CNMs, including NDs, can be used in bone/tissue engineering [13]. The authors reported the beneficial contribution of the NDs thanks to their enhanced mechanical properties and biocompatibility, as evidenced by the positive immune response toward the implanted composites. Another group from Lelkes' team investigated octadecylamine (ODA)-functionalized ND–poly(L-lactic acid) (PLLA) composites [70] in 2011. The mechanical properties showed a 4-fold improvement in material hardness. Experiments using osteogenic marker gene expression demonstrated that both NDs and NDs-ODA are nontoxic to murine osteoblasts and are able to support *in vitro* cell proliferation. The combination of these properties, including biocompatibility, good dispersion, good affinity and intrinsic fluorescence, has made ND-ODA-PLLA composites promising materials for bone tissue engineering and regenerative medicine. Another group aimed to develop a new construct based on a three-dimensional (3D) β-tricalcium phosphate (β-TCP) scaffold and angiopoietin-1 (ANG-1) immobilized onto NDs to provide a sufficient vascularization (e.g., for nutrients and oxygenation supplies) within bone substituents [71]. Their results demonstrated that such scaffolds was a valuable method to improve the features of implants (30-fold increase in the active surface area) and was of great interest for some new approaches attended for bone tissue engineering [71].

4.2 Labeling: NDs as bioimaging contrast agents

4.2.1 NDs as fluorescent biomarkers

Nitrogen atoms are the major impurities present in the diamond crystal lattice. Natural defects such as nitrogen vacancy (NV) centers have been used as stable natural sources of fluorescent color centers under appropriate light excitation [10]. These nitrogen-based centers correspond to the substitution of a carbon atom with a nitrogen atom bound to a lattice vacancy in the diamond structure and absorb in the ultraviolet (UV)–visible wavelength range of 460–600 nm. Negatively charged NV (NV^-) defects (uncoupled electron spin, $S = 1$, paramagnetic) fluoresce in red. Besides, it should be mentioned that other vacancy defects (i.e., EuV, SiV, BV and GeV) have some interesting optical properties which contribute to several emerging applications (e.g., quantum technologies, nanoscale sensing, photoluminescent biomarkers) [10]. Some fluorescent defects in NDs are derived from the starting material by explosive production during ND production. The HPHT technique yields particles more suitable for fluorescence since these particles have a high crystalline structure. The resulting particles contain a higher density of fluorescent centers than DET NDs and display good long-term photostability. Therefore, HPHT NDs are often referred to as "fluorescent nanodiamonds" (FNDs), the material of choice for fluorescent sensing or labeling applications because of their better optical properties. In this case, the density is higher than 10 ppm (1 ppm = 10^{-6}) [67]. The nitrogen content is determined by combustion analysis, and the nitrogen location within the samples is achieved by electron energy loss spectroscopy (EELS) measurements [6]. For NDs with negligible nitrogen-doped center concentrations, doping NDs with high-energy particle beams (electrons, protons, helium ions) and annealing creates additional NV color centers through vacancy migration [5,10,93].

Among various exogeneous optical contrast agents, FNDs have recently emerged as an attractive option to provide a highly stable platform for specific fluorescence bioimaging applications while leaving the surface available for further functionalization with biological targets and drugs [94]. In addition, compared to conventional dyes, NDs do not overcome photobleaching; therefore, NDs are suitable for long-term experiments. Near-infrared (NIR) fluorescence microscopy and imaging included in therapeutic windows allow *in vivo* experiments in tissue with 3 cm resolution [95]. Li and colleagues found that NDs are promising candidates for cell tracking [87]. FNDs, typically HPHT particles, coupled to molecules to track or potentially transport drugs, have been developed to monitor drug release within the body. Su et al. suggested coating 100 nm FNDs with human serum albumin (HSA) by passive adsorption and characterized their system by

magnetically modulated fluorescence imaging (excitation 530 nm; emission 670 nm) for cell therapy applications. Consequently, they presented their platform for quantitative monitoring of human placenta choriodecidual membrane-derived mesenchymal stem cells (pcMSCs) in miniature pigs by magnetic modulation [96]. They were able to visualize FND-labeled pcMSCs transplanted into the animal's organs and tissues after i.v. administration. Similarly, Zhang et al. focused on developing a highly stabilized ND system for fluorescent labeling [82]. Their FND·dBSA-PEG3000-biotin system was developed using a bottom-up approach to ensure a reliable surface modification strategy that enables stabilizing electrostatic and hydrophobic interactions. The design consists of an amphiphilic biopolymer derived from denatured bovine serum albumin (dBSA) with covalently grafted PEG chains terminated with biotin (TEM size: 150 nm). Their application of fluorescent NDs is considered a nontoxic alternative to quantum dots for medical imaging.

Alternatively, the use of external contrast agents could significantly improve the sensitivity of the technique. NIR labeling can be achieved by conjugating NDs with NIR dyes (e.g., Oregon Green [81], folic acid (FA)) or by using electrostatic interactions (e.g., cyanine). For this approach, both DET and HPHT NDs were used. In studies by Meinhardt and coworkers, the inherent surface chemistry of NDs allowed the introduction of a linker to enable "click" reactions with green dyes [81]. This strategy allowed the preparation of a probe labeled with fluorescent molecules and biological vectors for advanced applications such as luminescent molecular imaging.

4.2.2 NDs for photoacoustic microscopy

Photoacoustic (PA) imaging, which is an emerging preclinical modality, provides increased depth penetration for *in vivo* visualization [97]. The prospective application of NDs has been explored due to their optical absorbance. NDs absorb laser energy and convert it into heat that undergoes thermoelastic expansion and ultrasonic waves. Zhang et al. prepared a specific breast cancer detection method using NDs as a PA imaging contrast agent [72]. The surface of the NDs was grafted with PEG and then conjugated to an affinity ligand, an anti-HER2 peptide, to target HER2-positive overexpressing breast cancer cells. ND-based platforms (92 nm) were administered to BALB/C mice bearing HER2-positive and HER2-negative tumors. PA imaging of the NDs-PEG-anti-HER2 peptide *in vivo* enabled tumor localization by active targeting of HER2 cancer cells.

4.2.3 Lanthanide complexes-NDs for MRI

MRI is one of the most widely applied medical techniques because it provides high-contrast mapping images of organisms for the detection of affected tissues. MRI requires radio frequency (RF) and high magnetic fields while producing images with high spatial resolution and deep tissue penetration [98]. Image contrast relies on water proton ^{1}H NMR signals with intensities proportional to relaxation rates ($R_{1,2}$) of the nuclear spins, concentrations and environments of water molecules in the tissues. Thus, contrast agents (CAs) are usually used to enhance the local signal intensity by increasing the number of polarized spins. These agents mainly consist of paramagnetic metal species coordinated to organic macrocycles (i.e., Gd(III) or Mn(II/III) complexes), resulting in a decrease in T_1 (longitudinal relaxation time) [98]. It is recognized that the relaxivity of a lanthanide-based CA can be improved by optimizing the inner-sphere relaxivity mechanism by slowing down the tumbling of chelates. A common strategy consists of combining a gadolinium-based complex with nanoscale particles [99–102]. Functional groups (i.e., carboxylic acids) on the DET ND surface allow direct grafting of conventional amine-functionalized Gd(III) chelates to form a system detectable by MRI (Table 2 [73–75,103–105]). Manus and coworkers showed that conjugated Gd^{3+}(DO3A)-NDs exhibited higher relaxivity than conventional CAs due to intrinsic parameters of the considered system (i.e., influence of rotational correlation time, τ_R) [73,106]. The increase of per-Gd^{3+} relaxivity (1.5 T, 60 MHz) reached 988% (r_1: (58.82±1.18) $s^{-1}\cdot mmol^{-1}\cdot L$) compared with the relaxivity of the single Gd^{3+}(DO3A) complex (r_1: 5.4 $s^{-1}\cdot mmol^{-1}\cdot L$), as shown in the T_1-weighted phantoms (Fig. 4).

Before conjugation, NDs had a hydrodynamic diameter of approximately 21 nm, whereas Gd^{3+}(DO3A)-NDs formed aggregates (128 nm). It was suggested that Gd^{3+}(DO3A)-ND aggregations contribute to the increase in longitudinal relaxivity. Cell viability assays on human ovary adenocarcinoma (SKOV-3) cells revealed no significant cytotoxic effect. In 2016, *in vivo* imaging experiments were performed to monitor cancer growth in mice with a Gd-ND system at a high magnetic field [103]. Rammohan et al. suggested grafting Gd^{3+}(DO3A)-C_5-COOH (r_1: 6.4 $s^{-1}\cdot mmol^{-1}\cdot L$ at 1.4 T and 37 °C) onto an

Table 2 Summary of modified NDs for biolabeling applications as potential $T_{1/2}$-weighted contrast agents for MRI in aqueous solution [73–75,103–105]

System	D/nm	r_1/($s^{-1}\cdot mmol^{-1}\cdot L$)	η/%	Experimental conditions		Ref.
				B/T	t/°C	
DET ND-C_6-Gd^{3+}(DO3A)·H_2O	128 [a)]	58.8 (5.4 [c)])	988	1.5	37	[73]
DET ND-Si-C_5-Gd^{3+}(DO3A)·H_2O	75	11.1 (6.4 [d)])	73	1.4	37	[103]
		11.5 (4.8 [d)])	139	7	37	
DET ND-Gd^{3+}	7 [b)]	33.4 (4.8 [e)])	596	8	37	[74,104]
DET ND-PG-Gd^{3+}(DTPA)·H_2O	51	19.4 (3.7 [f)])	424	1.5	uk	[75]
		16.7 (3.5 [f)])	377	3	uk	
		8.2 (3.4 [f)])	141	7	uk	
DET ND-Mn^{2+}(EDTA)·H_2O	65	22.7 (1.7 [g)])	1235	7	uk	[105]

a) Number intensity. b) Volume intensity. c) Gd-DO3A. d) Gd-DO3A-C_5-COOH. e) Gd-BOPTA. f) Gd-DTPA. g) Mn-EDTA.
Notes: D is the hydrodynamic diameter size in water; r_1 is the per-Gd(III) relaxivity reflecting the efficiency of a contrast agent to reduce the longitudinal relaxation time of water protons; η is the relative enhancement of r_1; B is the magnetic field; t is the temperature; DET, detonation; DO3A, a gadoteridol macrocycle; DTPA, diethylenetriaminepentaacetic acid, a linear chelator; EDTA, ethylenediamine tetraacetic acid, a linear ligand; ND, nanodiamond; PG, polyglycerol; "uk" indicates "unknown" if the information is not mentioned either in the paper or in the corresponding supporting information; Gd^{3+}/Mn^{2+} chelates are associated to a single water molecule coordinated to the paramagnetic center (e.g., Gd^{3+} and Mn^{2+}).

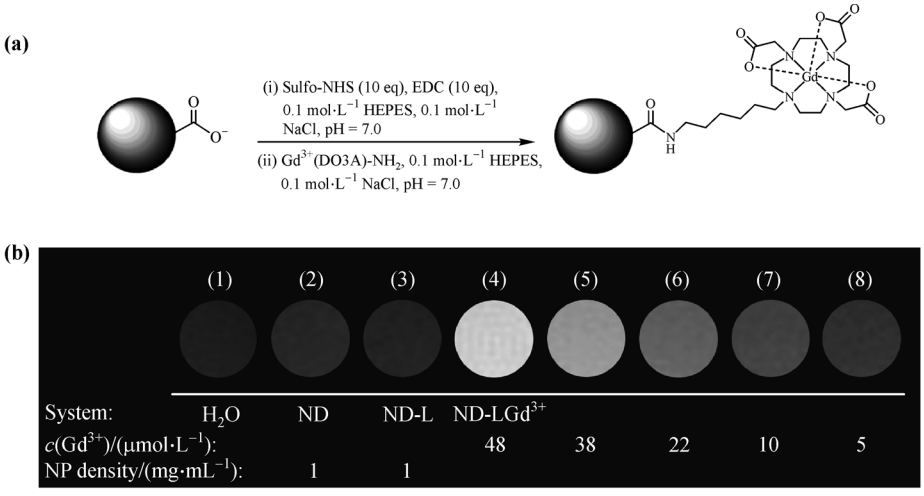

Fig. 4 **(a)** Structural ND platform of Gd^{3+}(DO3A)-NDs with Gd(III) chelates conjugated to the particle surface (hydrodynamic diameter of 128 nm). **(b)** MRI phantoms of samples: (1) water; (2) 1 mg·mL^{-1} DET NDs; (3) DET NDs conjugated to chelate (L) without gadolinium ion complexation (ND-L); DET NDs conjugated to Gd(III) chelate (ND-LGd^{3+}) with Gd^{3+} concentrations of (4) 48 μmol·L^{-1}, (5) 38 μmol·L^{-1}, (6) 22 μmol·L^{-1}, (7) 10 μmol·L^{-1}, and (8) 5 μmol·L^{-1}. Reproduced with permission from Ref. [73] (Copyright American Chemical Society, 2010).

amino-functionalized ND surface. DET NDs were reduced by borane followed by silanization with p-aminophenyltrimethoxysilane (APTS) to conjugate carboxylated Gd(III) chelates. Their system showed a 73% increase in longitudinal relaxivity (D_h: 75 nm; r_1: 11.1 $s^{-1}\cdot mmol^{-1}\cdot L$) [103]. Recently, a different approach relying on the absence of a Gd^{3+}-based complex against Gd^{3+} ions themselves was designed using a suspension of DET NDs modified with paramagnetic cations prepared from metal nitrates [74,104]. Panich's group reported the preparation of Gd(III) ion-grafted NDs in which the interaction is assumed to occur by exchange with protons from the carboxylic acid functional groups on the NDs to the Gd^{3+} prepared with $Gd(NO_3)_3\cdot 6H_2O$ [74]. Their system demonstrated high relaxivity values (D_h: 7 nm in volume; r_1: 33.4 $s^{-1}\cdot mmol^{-1}\cdot L$; r_2: 332 $s^{-1}\cdot mmol^{-1}\cdot L$ at 8 T and 37 °C) compared with MR relaxivity and phantom imaging (3 T). To determine the corresponding Gd(III) contribution of the spin-lattice (r_1) and spin–spin (r_2) relaxivities of such a system, they removed the intrinsic background of the NDs. Through a combination of characterization tools (EPR and ^{1}H NMR), it appeared that two to five Gd(III) ions were

anchored per particle according to their experimental conditions. Furthermore, Zhao and collaborators have reported a sophisticated strategy to design DET ND-PG-Gd^{3+}(DTPA) through multistep organic transformations, leading to a system that demonstrated good dispersibility in addition to high relaxometric properties [75]. Due to the potential toxicity of free gadolinium ions, Hou and co-workers in 2017 proposed using manganese ions (Mn^{2+}) as an alternative. His group constructed different functionalized ND systems with a Mn(II) chelating agent attached on the ND surface using ligand derivatives to develop Mn^{2+}(EDTA)-ND or Mn^{2+}(DOTA)-ND MRI CAs [105]. The resulting Mn(II)-labeled platforms were found to improve sensitivity during *in vitro* and *in vivo* assays. In addition, they were able to decrease longitudinal and transversal relaxation by optimizing both T_1- and T_2-weighted MRI as a dual probe to improving liver tumor diagnosis.

4.2.4 MRI applications with hyperpolarized NDs

Among the recent approaches, the hyperpolarization technique of paramagnetic compounds was expected to considerably improve the distribution of spin states. By using the Overhauser effect, a transfer of electron polarization to the nuclear spins (e.g., ^1H or ^{13}C) can be obtained under microwave irradiation to induce a spin polarization that can lead to a strong increase in protons or ^{13}C.

While some paramagnetic structures have been explored for this purpose (e.g., organic TEMPO derivatives) [77,107–108], the use of NDs can be relevant for either MRI or Overhauser MRI (OMRI) due to the intrinsic properties of NDs. This novel approach allows for high contrast on MR imaging through *in situ* hyperpolarization at an ultralow magnetic field (ULF) [77]. NDs exhibit paramagnetic impurities mainly due to structural defects (radical-like paramagnetic centers (RPCs), as unpaired electron spins of disordered dangling C−C bonds, P1, NV). Dynamic nuclear polarization (DNP), as a hyperpolarization technique, can provide efficient polarization transfer from these electrons to neighboring nuclei. This achievement can thus occur through an electron-nuclear cross relaxation process when the electron spin polarization deviates from the equilibrium state by microwave (MW) irradiation (Fig. 5). Imaging experiments were established using radio frequency (RF; approximately 190 MHz) excitation in a regime compatible with biological study and at ULF (6 mT) to maximize efficient nuclear polarization

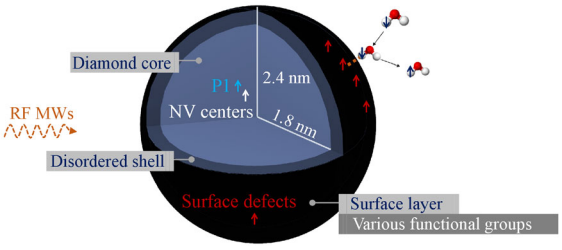

Fig. 5 Schematic representation of the intrinsic properties of NDs and the Overhauser effect based on ND impurities (NDs and nearby water molecules). Paramagnetic contributions from surface defects and core centers. RF MWs, radio frequency microwaves; P1, substituted nitrogen defect centers, NV^-; NV, nitrogen-vacancy centers.

while creating an on/off contrast. Indeed, the detectable contrast can be visualized as a continuous transfer of surface-localized RPCs to ^1H nuclei from water during the RF pulse of electron paramagnetic resonance (EPR) transition between MRI acquisitions [77–78].

HPHT NDs ranging in size from 18 to 125 nm and polycrystalline DET NDs (100 mg·mL^{-1}) were studied by DNP and EPR spectroscopy, and both types were detectable under these conditions. The hyperpolarized particles were also visualized in high contrast sensitivity (threshold: 1 mg·mL^{-1}) gray level phantom images. In addition, it may be noted that air annealing prior to surface modification tends to decrease the amplitude of the broad signal component in the EPR spectra [79]. Waddington et al. also reported the design, construction and experiment of potential *in vivo* imaging applications of NDs as a practical screening methodology for long-term application [77]. Additionally, this new setup reduces maintenance costs since the new methodology does not require high magnetic fields.

Alternatively, NDs can be detected by acquiring signals from ^{13}C nuclei using RPC in diamond hyperpolarization transferred to ^{13}C nuclei using microwaves [79]. In fact, the long relaxation times of ^{13}C (1/2) spins in diamond are naturally obtained. Recent studies have reported the use of NDs for hyperpolarized ^{13}C MRI to improve $T_{1/2}$ by enhancing ^{13}C polarization by DNP [76,79,109–112]. Hyperpolarized imaging was clearly observed in phantoms and *in vivo* imaging using 2 μm particles as CAs after intrathoracic injection of a mouse [79]. The image was superimposed on the corresponding ^1H MR image to provide anatomical features. In 2020, Boele et al. identified the contribution of RPCs, such as substituted nitrogen (P1) centers, to ^{13}C nuclei and their roles in DNP experiments [112]. These achievements open up new opportunities for

NDs in bioimaging, suggesting versatile developments as new hyperpolarizing agents for MRI [113–114].

4.3 Agents for delivery: NDs as carriers for the delivery of agents in cancer therapy

One of the major trends in cancer therapy research is the ability of a carrier to release small chemical drugs to specific diseased cells or tissues, possibly while tracking their location in the body through exogeneous contrast agents (i.e., theranostic probes). This so-called 'drug delivery' process relies on the optimization of molecule transport by a nanocarrier to deliver anticancer drugs to appropriate tissues. This process allows a stable carrier in the bloodstream to gradually release drugs adsorbed on the nanostructure or by noncovalent encapsulation in nanostructures (i.e., mesoporous particles, micelles, liposomes). Strategies for ND-based drug delivery design are achieved by (i) drug deposition onto the ND surface through electrostatic interactions and hydrogen bonds or by (ii) covalent attachment to ND functional groups sensitive to acidic environments.

4.3.1 Small drugs delivery with NDs

ND-based systems are an attractive option for specific applications in cancer therapy, such as nanocarriers for drug delivery. Their attractive optical properties (red emission) enable long-term monitoring of the drug delivery process into cancer cells. For example, the common DOX chemotherapeutic drug exhibits anticancer activity by inducing apoptotic death of abnormally divided cells. It appears that chemotherapeutic drugs are highly cytotoxic and can cause serious side effects because of their lack of specificity. The anticancer drug can be loaded onto (fluorescent) (F)NDs through physical adsorption (ND·DOX complexes). The combination of carriers and drugs keep the free DOX concentration below a toxic level for normal tissues by releasing DOX over a long time. Dean Ho's team developed a simple and efficient procedure based on the adsorption of hydrophobic chemodrugs on NDs (DOX; epirubicin (EPI); bleomycin (BLEO); paclitaxel (PAC); mitoxantrone (MTX)) [7]. Prolonged release of DOX from ND platforms significantly increased unhealthy cell apoptosis in mouse models, preventing tumor growth suppression more efficiently than conventional treatment. In addition, according to Chow et al., NDs coupled with DOX prevent the system from being pumped out of cells [83]. Experiments focused on a first-generation drug delivery ND platform for breast cancer (4T1 cells) and liver cancer (LT2-M cells) with promising results in tumor retention and increased blood flow half-life compared with unmodified DOX activity. Merkel et al. established the activity mode of the release of DOX through ND-mediated delivery [115]. Figure 6 shows the cellular uptake and efficient drug release using a PEGylated platform (Fig. 6) [116].

Liu et al. achieved different covalent binding of paclitaxel to the ND surface by a succession of chemical modifications [85]. As observed, the platform reduced cell viability in A549 human lung carcinoma cells. Further-

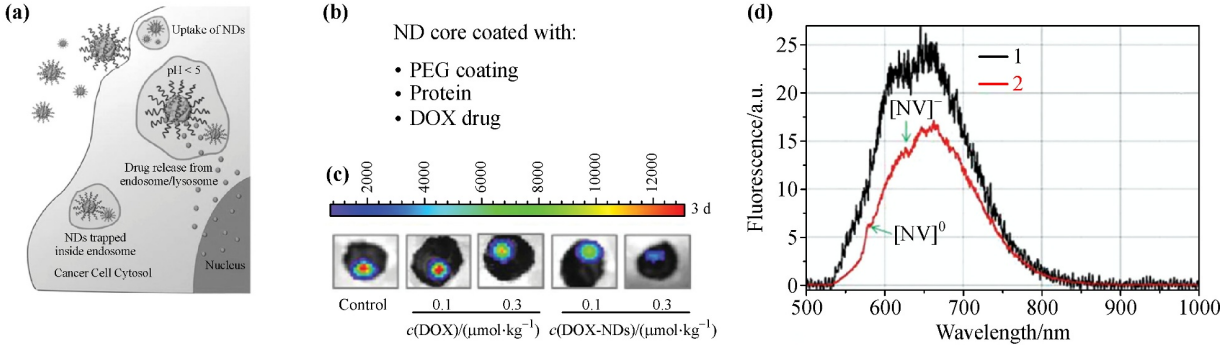

Fig. 6 **(a)** Schematic representation of cell uptake and the antitumor drug release process of NDs as a delivery system for DOX from into two phases: the mechanism enabling particle uptake into the cell (endocytosis) to release the drug, and then the diffusion of the free drug. **(b)** Schematic fluorescent ND·DOX platform with a ND core, protein coating (human serum albumin, HSA) and NHS-PEG2000. **(c)** Photos of the tumor extracted from a breast cancer xenograft in the chorioallantoic membrane (CAM) model. After two different treatments for 3 d *in vivo*, from left to right: controls (PBS), only DOX, and DOX coupled NDs. According to the results, the ND-DOX system inhibits tumor growth efficiently by decreasing the viability of human cancer (MDA-MB-231 breast cancer). These breast cancer cells stably expressing firefly luciferase were attached to chicken embryo CAM. ND-DOX inhibited the bioluminescence of transgenic tumors stably expressing luciferase, resulting in an inhibition of tumor growth. This effect was greater than that induced by free DOX. **(d)** Emission spectrum after laser excitation: (1) overlapping of NV centers of ND and DOX, and (2) ND optical properties after laser bleaching (NV centers, 575 nm and NV^-, 638 nm). Reproduced with permission from Ref. [116] (Copyright John Wiley and Sons, 2015).

more, ND-PAC blocked tumor growth *in vivo* (SCID mice) and the formation of lung cancer cells using xenografts. PAC acts by blocking microtubules to mediate mitotic arrest in cancer cells. Gismondi et al. reported the adsorption of secondary plant metabolites (ciproten and quercetin) onto NDs that penetrated the cell cytoplasm [117]. These chemotherapeutic systems showed antiproliferative effects on human (HeLa) and murine (B16F10) tumor cells.

A second generation is based on the covalent functionalization of NDs with polymeric chains for small drug delivery and slow release. This approach has been used by different teams to improve dispersion in physiological media and has led to the conclusion that this delivery strategy can indeed provide efficient drug transport into cancer cells. Wang et al. adsorbed DOX hydrochloride onto PEGylated red fluorescent NDs (140 nm in size) and showed promising results for *in vitro* and in cell culture with human liver cancer cells (HepG2 cells) [84]. PEGylated NDs were prepared via a multistep organic transformation of carboxylic acids to acyl chloride intermediates, leading to a platform of DOX-coupled PEG-OH NDs. It was observed that, the NDs entered the cells and enhanced drug uptake. Another approach by Zhang et al. involved polyPEGylation of ND by surface-initiated atom transfer radical polymerization using PEGMA475 as a monomer [118]. Intracellular delivery of DOX using polyPEGylated NDs has been studied in more detail. According to their work, a cell internalization study revealed that NDs facilitated drug transport in A549 cells. Li et al. obtained a different ND-PEG nanocarrier by coupling NH_2-PEG-COOH onto carboxylated NDs (140 nm) with adsorption of DOX and tested it on cultures (HepG2, HeLa and MCF-7 cells) [64]. These agents were designed for pH-sensitive release. Since the pH of blood and normal tissue is approximately 7.4 and is much lower in the tumoral environment (pH 5), the efficient ND-PEG·DOX drug delivery system was able to release DOX.

For polymer-modified NDs, PEG was introduced onto NDs not only to improve the colloidal stability of the suspension but also to increase the clearance time and prolong blood circulation time by reducing nonspecific interactions (e.g., with cells). Nevertheless, a major drawback of these chemotherapeutic systems is their lack of selective recognition of tumor cells compared to normal cells, leading to potential side effects during the treatment process. Therefore, tumor-targeted ND carriers have been developed to selectively carry nonspecific cytotoxic drugs into pathologic cells. This concept of a vectorized ND platform was introduced by various teams, including Dong and coworkers [86]. His group synthesized modified NDs with PEG-diamine conjugation with folate (FA) [119], forming an ND-PEG-FA nanocarrier system. DOX was physically attached to PEGylated NDs-FA. Their system showed excellent stability under neutral pH conditions and loaded a large amount of drug in an acidic environment. Similarly, conjugation of DOX·ND with the cell-penetrating TAT peptide could enhance intracellular drug release and block premature delivery [87]. Several other approaches have been reported, such as PEGylated ND sensors to track and transmit drug release to cells [120]. Zhao et al. reported a sophisticated strategy to increase solubility using a polyglycerol coating [75]. They developed a DET ND-PG-Gd(III) platform through multistep organic transformations and demonstrated good dispersibility in PBS, efficient functionalization and an attractive potential carrier for drug-coupled theranostic applications. Other strategies to prevent aggregation were discussed, including NDs coated with albumin-derived polymer and an HSA-derived biopolymer that loads drugs [121].

4.3.2 Gene or protein/peptide delivery

Zhang and coworkers reported the delivery of plasmid DNA using NDs covered with 800 Da polyethyleneimine (PEI800) [88]. First, the highly positively charged PEI800 polymer was loaded onto acid-treated NDs. Then, the ND-based system was able to bind to negatively charged DNA through electrostatic interactions. As expected, the agent exhibited higher gene transfection efficiency with low cytotoxicity. Current limitations associated with the nonspecific nature of many drugs limit the potential of chemotherapy. An alternative approach is antibody (Ab) therapy, as suggested by Smith and collaborators [122]. ND-Ab systems were found to be stable in a biological environment and trigger the release of active Abs under extreme physiological conditions. Other groups have demonstrated that oxidized NDs have a high affinity for different types of molecules, including proteins, such as myoglobin and albumin [123].

5 Conclusions

This review aimed to highlight the place of NDs for preclinic biomedical applications such as cancer therapy, labeling and targeting drug delivery. Detonation and HPHT

NDs are considered some of the most attractive carbon-based materials, as the synthesis methodology allows for large-scale production by a low-cost process. Overall, NDs are formed by sp^3 carbon atoms in the core surrounded by an sp^2 shell with other impurity atoms on the surface that provide both a reservoir of electrons and inherent surface chemistry for grafting versatile probes. All their remarkable characteristics provide stable intrinsic properties, such as biological, optical, magnetism, and functionalization features. Thus, NDs can be explored as useful labels in different imaging modalities and used to monitor and mediate drug delivery. Despite their numerous advantages, NDs have to overcome some limitations such as low intrinsic fluorescence from color centers. Taking into account the broad range of NDs production methods and the correlated NDs physicochemical properties (e.g., surface, crystallinity, size, NDs doping by ion implantation following by annealing), the optical properties can be optimized. A key challenge in diagnostic applications lies in intrinsic features and surface modifications, while a good understanding of surface chemistry for theranostic applications could afford *in vivo* tracking. In addition, current challenges provide a wide range of directions as powerful MRI CA for exploring new approaches using OMRI mechanisms or ^{13}C MRI due to hyperpolarization techniques. Some additional research directions are yet to be explored to ensure optimal and appropriate use of NDs.

Disclosure of potential conflicts of interest The authors declare that they have no conflict of interest.

Acknowledgements The authors thank the Center for Microscopy and Molecular Imaging (CMMI, supported by the European Regional Development Fund and Wallonia), the Fond National de la Recherche Scientifique (FNRS), the Actions de Recherche Concertées (ARC) programs of the French Community of Belgium, COST actions and the Walloon region. The authors would like to acknowledge the Interuniversity Attraction Poles of the Belgian Federal Science Policy Office and the European Union's Horizon 2020 research and innovation programme under grant agreement No. 863099.

References

[1] Tsakalakos T, Ovid'ko I A, Vasudevan A K, eds. Nanostructures: Synthesis, Functional Properties and Applications. Springer Netherlands, 2003

[2] Bae K H, Chung H J, Park T G. Nanomaterials for cancer therapy and imaging. Molecules and Cells, 2011, 31(4): 295–302

[3] Jeevanandam J, Barhoum A, Chan Y S, et al. Review on nanoparticles and nanostructured materials: History, sources, toxicity and regulations. Beilstein Journal of Nanotechnology, 2018, 9: 1050–1074

[4] Afandi A, Howkins A, Boyd I W, et al. Nanodiamonds for device applications: An investigation of the properties of boron-doped detonation nanodiamonds. Scientific Reports, 2018, 8(1): 3270–3280

[5] Yang N, ed. Novel Aspects of Diamond: From Growth to Applications. 2nd ed. Cham, Switzerland: Springer Nature Switzerland AG, 2019

[6] Turner S, Lebedev O I, Shenderova O, et al. Determination of size, morphology, and nitrogen impurity location in treated detonation nanodiamond by transmission electron microscopy. Advanced Functional Materials, 2009, 19(13): 2116–2124

[7] Ho D, ed. Nanodiamonds: Applications in Biology and Nanoscale Medicine. Springer US, 2010

[8] Devasena T. Therapeutic and Diagnostic Nanomaterials. Springer Singapore, 2017

[9] Donnet C, Erdemir A, eds. Tribology of Diamond-like Carbon Films: Fundamentals and Applications. Springer US, 2008

[10] Ashfold M N R, Goss J P, Green B L, et al. Nitrogen in diamond. Chemical Reviews, 2020, 120(12): 5745–5794

[11] Bogatyreva G P, Marinich M A, Ishchenko E V, et al. Application of modified nanodiamonds as catalysts of heterogeneous and electrochemical catalyses. Physics of the Solid State, 2004, 46(4): 738–741

[12] Lai H, Stenzel M H, Xiao P. Surface engineering and applications of nanodiamonds in cancer treatment and imaging. International Materials Reviews, 2020, 65(4): 189–225

[13] Eivazzadeh-Keihan R, Maleki A, de la Guardia M, et al. Carbon based nanomaterials for tissue engineering of bone: building new bone on small black scaffolds: A review. Journal of Advanced Research, 2019, 18: 185–201

[14] Grausova L, Bacakova L, Kromka A, et al. Nanodiamond as promising material for bone tissue engineering. Journal of Nanoscience and Nanotechnology, 2009, 9(6): 3524–3534

[15] Chauhan S, Jain N, Nagaich U. Nanodiamonds with powerful ability for drug delivery and biomedical applications: Recent updates on *in vivo* study and patents. Journal of Pharmaceutical Analysis, 2020, 10(1): 1–12

[16] Balek L, Buchtova M, Kunova Bosakova M, et al. Nanodiamonds as "artificial proteins": Regulation of a cell signalling system using low nanomolar solutions of inorganic nanocrystals. Biomaterials, 2018, 176: 106–121

[17] Liu Y Y, Chang B M, Chang H C. Nanodiamond-enabled biomedical imaging. Nanomedicine, 2020, 15(16): 1599–1616

[18] Terada D, Genjo T, Segawa T F, et al. Nanodiamonds for bioapplications — Specific targeting strategies. Biochimica et Biophysica Acta: General Subjects, 2020, 1864(2): 129354

[19] Panich A M, Sergeev N A, Shames A I, et al. Size dependence of ^{13}C nuclear spin-lattice relaxation in micro- and nanodiamonds. Journal of Physics: Condensed Matter, 2015, 27(7): 072203

[20] Gruen D M, Shenderova O A, VulA, eds. Synthesis, Properties and Applications of Ultrananocrystalline Diamond. Springer, 2005, 192: 241–252

[21] Tamburri E, Orlanducci S, Reina G, et al. Nanodiamonds: The ways forward. In: Rossi M, Dini L, Passeri D, et al., eds. Nanoforum 2014, 2015, 1667: 020001

[22] Khachatryan A Kh, Aloyan S G, May P W, et al. Graphite-to-diamond transformation induced by ultrasound cavitation. Diamond and Related Materials, 2008, 17(6): 931–936

[23] Butler J E, Sumant A V. The CVD of nanodiamond materials. Chemical Vapor Deposition, 2008, 14(7–8): 145–160

[24] Arnault J C, ed. Nanodiamonds: Advanced Material Analysis, Properties and Applications. Elsevier, 2017

[25] Barnard A S. Stability of diamond at the nanoscale. In: Shenderova O A, Gruen D M, eds. Ultananocrystalline Diamond. 2nd ed. Elsevier, 2012, 3–52

[26] Dolmatov V Y. Detonation nanodiamonds: Synthesis, structure, properties and applications. Uspekhi Khimii, 2007, 76(4): 375–397

[27] Osswald S, Yushin G, Mochalin V, et al. Control of sp^2/sp^3 carbon ratio and surface chemistry of nanodiamond powders by selective oxidation in air. Journal of the American Chemical Society, 2006, 128(35): 11635–11642

[28] Mochalin V N, Shenderova O, Ho D, et al. The properties and applications of nanodiamonds. Nature Nanotechnology, 2012, 7(1): 11–23

[29] Pentecost A, Gour S, Mochalin V, et al. Deaggregation of nanodiamond powders using salt- and sugar-assisted milling. ACS Applied Materials & Interfaces, 2010, 2(11): 3289–3294

[30] Peristyy A A, Fedyanina O N, Paull B, et al. Diamond based adsorbents and their application in chromatography. Journal of Chromatography A, 2014, 1357: 68–86

[31] Rehor I, Slegerova J, Kucka J, et al. Fluorescent nanodiamonds embedded in biocompatible translucent shells. Small, 2014, 10(6): 1106–1115

[32] Reina G, Zhao L, Bianco A, et al. Chemical functionalization of nanodiamonds: Opportunities and challenges ahead. Angewandte Chemie International Edition, 2019, 58(50): 17918–17929

[33] Boudou J P, Curmi P A, Jelezko F, et al. High yield fabrication of fluorescent nanodiamonds. Nanotechnology, 2009, 20(23): 235602–235613

[34] Schrand A M, Huang H, Carlson C, et al. Are diamond nanoparticles cytotoxic? The Journal of Physical Chemistry B, 2007, 111(1): 2–7

[35] Spitsyn B V, Gradoboev M N, Galushko T B, et al. Purification and functionalization of nanodiamond. In: Gruen D M, Shenderova O A, Vul A, eds. Synthesis, Properties and Applications of Ultrananocrystalline Diamond. Springer, 2005, 192: 241–252

[36] Choi E Y, Kim K, Kim C K, et al. Reinforcement of nylon 6,6/nylon 6,6 grafted nanodiamond composites by *in situ* reactive extrusion. Scientific Reports, 2016, 6(1): 37010–37020

[37] Zhang X, Fu C, Feng L, et al. PEGylation and polyPEGylation of nanodiamond. Polymer, 2012, 53(15): 3178–3184

[38] Krueger A. The structure and reactivity of nanoscale diamond. Journal of Materials Chemistry, 2008, 18(13): 1485–1492

[39] Jariwala D H, Patel D, Wairkar S. Surface functionalization of nanodiamonds for biomedical applications. Materials Science and Engineering C, 2020, 113: 110996

[40] Shenderova O, Koscheev A, Zaripov N, et al. Surface chemistry and properties of ozone-purified detonation nanodiamonds. The Journal of Physical Chemistry C, 2011, 115(20): 9827–9837

[41] Ackermann J, Krueger A. Efficient surface functionalization of detonation nanodiamond using ozone under ambient conditions. Nanoscale, 2019, 11(16): 8012–8019

[42] Kume A, Mochalin V N. Sonication-assisted hydrolysis of ozone oxidized detonation nanodiamond. Diamond and Related Materials, 2020, 103: 107705–107711

[43] Ackermann J, Krueger A. Highly sensitive and reproducible quantification of oxygenated surface groups on carbon nanomaterials. Carbon, 2020, 163(163): 56–62

[44] Heyer S, Janssen W, Turner S, et al. Toward deep blue nano hope diamonds: Heavily boron-doped diamond nanoparticles. ACS Nano, 2014, 8(6): 5757–5764

[45] Sun Y, Olsén P, Waag T, et al. Disaggregation and anionic activation of nanodiamonds mediated by sodium hydride — A new route to functional aliphatic polyester-based nanodiamond materials. Particle & Particle Systems Characterization, 2015, 32(1): 35–42

[46] Whitlow J, Pacelli S, Paul A. Multifunctional nanodiamonds in regenerative medicine: Recent advances and future directions. Journal of Controlled Release, 2017, 261(261): 62–86

[47] Krueger A, Stegk J, Liang Y, et al. Biotinylated nanodiamond: Simple and efficient functionalization of detonation diamond. Langmuir, 2008, 24(8): 4200–4204

[48] Bumb A, Sarkar S K, Billington N, et al. Silica encapsulation of fluorescent nanodiamonds for colloidal stability and facile surface functionalization. Journal of the American Chemical Society, 2013, 135(21): 7815–7818

[49] Jarre G, Liang Y, Betz P, et al. Playing the surface game — Diels–Alder reactions on diamond nanoparticles. Chemical Communications, 2011, 47(1): 544–546

[50] Lang D, Krueger A. The Prato reaction on nanodiamond: Surface functionalization by formation of pyrrolidine rings. Diamond and Related Materials, 2011, 20(2): 101–104

[51] Lang D, Krueger A. Functionalizing nanodiamond particles with N-heterocyclic iminium bromides and dicyano methanides. Diamond and Related Materials, 2017, 79: 102–107

[52] Girard H A, Arnault J C, Perruchas S, et al. Hydrogenation of nanodiamonds using MPCVD: A new route toward organic functionalization. Diamond and Related Materials, 2010, 19(7–9): 1117–1123

[53] Girard H A, El-Kharbachi A, Garcia-Argote S, et al. Tritium labeling of detonation nanodiamonds. Chemical Communications, 2014, 50(22): 2916–2918

[54] Nehlig E, Garcia-Argote S, Feuillastre S, et al. Using hydrogen isotope incorporation as a tool to unravel the surfaces of hydrogen-treated nanodiamonds. Nanoscale, 2019, 11(16): 8027–8036

[55] Claveau S, Nehlig É, Garcia-Argote S, et al. Delivery of siRNA to Ewing sarcoma tumor xenografted on mice, using hydrogenated detonation nanodiamonds: Treatment efficacy and tissue distribution. Nanomaterials, 2020, 10(3): 553

[56] Liu Y, Khabashesku V N, Halas N J. Fluorinated nanodiamond as a wet chemistry precursor for diamond coatings covalently bonded to glass surface. Journal of the American Chemical Society, 2005, 127(11): 3712–3713

[57] Lisichkin G V, Kulakova I I, Gerasimov Y A, et al. Halogenation of detonation-synthesised nanodiamond surfaces. Mendeleev Communications, 2009, 19(6): 309–310

[58] Bradac C, Osswald S. Effect of structure and composition of nanodiamond powders on thermal stability and oxidation kinetics. Carbon, 2018, 132: 616–622

[59] Xu X, Yu Z. Influence of thermal oxidation on as-synthesized detonation nanodiamond. Particuology, 2012, 10(3): 339–344

[60] Shenderova O, Petrov I, Walsh J, et al. Modification of detonation nanodiamonds by heat treatment in air. Diamond and Related Materials, 2006, 15(11–12): 1799–1803

[61] Apolonskaya I A, Tyurnina A V, Kopylov P G, et al. Thermal oxidation of detonation nanodiamond. Moscow University Physics Bulletin, 2009, 64(4): 433–436

[62] Gaebel T, Bradac C, Chen J, et al. Size-reduction of nanodiamonds via air oxidation. Diamond and Related Materials, 2012, 21: 28–32

[63] Sotoma S, Hsieh F J, Chen Y W, et al. Highly stable lipid-encapsulation of fluorescent nanodiamonds for bioimaging applications. Chemical Communications, 2018, 54(8): 1000–1003

[64] Li L, Tian L, Zhao W, et al. pH-sensitive nanomedicine based on PEGylated nanodiamond for enhanced tumor therapy. RSC Advances, 2016, 6(43): 36407–36417

[65] Terada D, Sotoma S, Harada Y, et al. One-pot synthesis of highly dispersible fluorescent nanodiamonds for bioconjugation. Bioconjugate Chemistry, 2018, 29(8): 2786–2792

[66] Wu Y Z, Weil T. Nanodiamonds for biological applications. Physical Sciences Reviews, 2017, 2(6): UNSP 20160104

[67] Prabhakar N, Rosenholm J M. Nanodiamonds for advanced optical bioimaging and beyond. Current Opinion in Colloid & Interface Science, 2019, 39: 220–231

[68] Dworak N, Wnuk M, Zebrowski J, et al. Genotoxic and mutagenic activity of diamond nanoparticles in human peripheral lymphocytes *in vitro*. Carbon, 2014, 68: 763–776

[69] Moche H, Paget V, Chevalier D, et al. Carboxylated nanodiamonds can be used as negative reference in *in vitro* nanogenotoxicity studies. Journal of Applied Toxicology, 2017, 37(8): 954–961

[70] Zhang Q, Mochalin V N, Neitzel I, et al. Fluorescent PLLA-nanodiamond composites for bone tissue engineering. Biomaterials, 2011, 32(1): 87–94

[71] Wu X, Bruschi M, Waag T, et al. Functionalization of bone implants with nanodiamond particles and angiopoietin-1 to improve vascularization and bone regeneration. Journal of Materials Chemistry B: Materials for Biology and Medicine, 2017, 5(32): 6629–6636

[72] Zhang T, Cui H, Fang C Y, et al. Targeted nanodiamonds as phenotype-specific photoacoustic contrast agents for breast cancer. Nanomedicine, 2015, 10(4): 573–587

[73] Manus L M, Mastarone D J, Waters E A, et al. Gd(III)-nanodiamond conjugates for MRI contrast enhancement. Nano Letters, 2010, 10(2): 484–489

[74] Panich A M, Salti M, Goren S D, et al. Gd(III)-grafted detonation nanodiamonds for MRI contrast enhancement. The Journal of Physical Chemistry C, 2019, 123(4): 2627–2631

[75] Zhao L, Shiino A, Qin H, et al. Synthesis, characterization, and magnetic resonance evaluation of polyglycerol-functionalized detonation nanodiamond conjugated with gadolinium(III) complex. Journal of Nanoscience and Nanotechnology, 2015, 15(2): 1076–1082

[76] Dutta P, Martinez G V, Gillies R J. Nanodiamond as a new hyperpolarizing agent and its ^{13}C MRS. The Journal of Physical Chemistry Letters, 2014, 5(3): 597–600

[77] Waddington D E J, Sarracanie M, Salameh N, et al. An Overhauser-enhanced-MRI platform for dynamic free radical imaging *in vivo*. NMR in Biomedicine, 2018, 31(5): e3896

[78] Waddington D E J, Sarracanie M, Zhang H, et al. Nanodiamond-enhanced MRI via *in situ* hyperpolarization. Nature Communications, 2017, 8(1): 15118–15127

[79] Waddington D E J, Boele T, Rej E, et al. Phase-encoded

hyperpolarized nanodiamond for magnetic resonance imaging. Scientific Reports, 2019, 9(1): 5950–5970

[80] Say J M, van Vreden C, Reilly D J, et al. Luminescent nanodiamonds for biomedical applications. Biophysical Reviews, 2011, 3(4): 171–184

[81] Meinhardt T, Lang D, Dill H, et al. Pushing the functionality of diamond nanoparticles to new horizons: Orthogonally functionalized nanodiamond using click chemistry. Advanced Functional Materials, 2011, 21(3): 494–500

[82] Zhang T, Neumann A, Lindlau J, et al. DNA-based self-assembly of fluorescent nanodiamonds. Journal of the American Chemical Society, 2015, 137(31): 9776–9779

[83] Chow E K, Zhang X-Q, Chen M, et al. Nanodiamond therapeutic delivery agents mediate enhanced chemoresistant tumor treatment. Science Translational Medicine, 2011, 3(73): 73ra21

[84] Wang D, Tong Y, Li Y, et al. PEGylated nanodiamond for chemotherapeutic drug delivery. Diamond and Related Materials, 2013, 36: 26–34

[85] Liu K K, Zheng W W, Wang C C, et al. Covalent linkage of nanodiamond-paclitaxel for drug delivery and cancer therapy. Nanotechnology, 2010, 21(31): 315106–315119

[86] Dong Y, Cao R, Li Y, et al. Folate-conjugated nanodiamond for tumor-targeted drug delivery. RSC Advances, 2015, 5(101): 82711–82716

[87] Li X, Shao J, Qin Y, et al. TAT-conjugated nanodiamond for the enhanced delivery of doxorubicin. Journal of Materials Chemistry, 2011, 21(22): 7966–7974

[88] Zhang X Q, Chen M, Lam R, et al. Polymer-functionalized nanodiamond platforms as vehicles for gene delivery. ACS Nano, 2009, 3(9): 2609–2616

[89] Purtov K, Petunin A, Inzhevatkin E, et al. Biodistribution of different sized nanodiamonds in mice. Journal of Nanoscience and Nanotechnology, 2015, 15(2): 1070–1075

[90] Inzhevatkin E, Baron A, Maksimov N, et al. Biodistribution of nanodiamonds in the body of mice using EPR spectrometry. IET Science, Measurement & Technology, 2019, 13(7): 984–988

[91] Suliman S, Mustafa K, Krueger A, et al. Nanodiamond modified copolymer scaffolds affects tumour progression of early neoplastic oral keratinocytes. Biomaterials, 2016, 95: 11–21

[92] Okamoto M, John B. Synthetic biopolymer nanocomposites for tissue engineering scaffolds. Progress in Polymer Science, 2013, 38(10–11): 1487–1503

[93] Chang Y R, Lee H Y, Chen K, et al. Mass production and dynamic imaging of fluorescent nanodiamonds. Nature Nanotechnology, 2008, 3(5): 284–288

[94] Parveen S, Misra R, Sahoo S K. Nanoparticles: A boon to drug delivery, therapeutics, diagnostics and imaging. Nanomedicine: Nanotechnology, Biology, and Medicine, 2012, 8(2): 147–166

[95] Dang X, Bardhan N M, Qi J, et al. Deep-tissue optical imaging of near cellular-sized features. Scientific Reports, 2019, 9(1): 3873–3885

[96] Su L J, Wu M S, Hui Y Y, et al. Fluorescent nanodiamonds enable quantitative tracking of human mesenchymal stem cells in miniature pigs. Scientific Reports, 2017, 7(1): 45607–45618

[97] Steinberg I, Huland D M, Vermesh O, et al. Photoacoustic clinical imaging. Photoacoustics, 2019, 14: 77–98

[98] Laurent S, Henoumont C, Stanicki D, et al. MRI Contrast Agents: From Molecules to Particles. Springer Singapore, 2017

[99] Lipani E, Laurent S, Surin M, et al. High-relaxivity and luminescent silica nanoparticles as multimodal agents for molecular imaging. Langmuir, 2013, 29(10): 3419–3427

[100] Guo C, Hu J, Bains A, et al. The potential of peptide dendron functionalized and gadolinium loaded mesoporous silica nanoparticles as magnetic resonance imaging contrast agents. Journal of Materials Chemistry B: Materials for Biology and Medicine, 2016, 4(13): 2322–2331

[101] Carniato F, Tei L, Botta M. Gd-based mesoporous silica nanoparticles as MRI probes: Gd-based mesoporous silica nanoparticles as MRI probes. European Journal of Inorganic Chemistry, 2018, 2018(46): 4936–4954

[102] Pellico J, Ellis C M, Davis J J. Nanoparticle-based paramagnetic contrast agents for magnetic resonance imaging. Contrast Media & Molecular Imaging, 2019, UNSP 1845637

[103] Rammohan N, MacRenaris K W, Moore L K, et al. Nanodiamond-gadolinium(III) aggregates for tracking cancer growth *in vivo* at high field. Nano Letters, 2016, 16(12): 7551–7564

[104] Osipov V Yu, Aleksenskiy A E, Takai K, et al. Magnetic studies of a detonation nanodiamond with the surface modified by gadolinium ions. Physics of the Solid State, 2015, 57(11): 2314–2319

[105] Hou W, Toh T B, Abdullah L N, et al. Nanodiamond-manganese dual mode MRI contrast agents for enhanced liver tumor detection. Nanomedicine: Nanotechnology, Biology, and Medicine, 2017, 13(3): 783–793

[106] Caravan P, Farrar C T, Frullano L, et al. Influence of molecular parameters and increasing magnetic field strength on relaxivity of gadolinium- and manganese-based T_1 contrast agents. Contrast Media & Molecular Imaging, 2009, 4(2): 89–100

[107] Dhas M K, Utsumi H, Jawahar A, et al. Dynamic nuclear polarization properties of nitroxyl radical in high viscous liquid using Overhauser-enhanced magnetic resonance imaging (OMRI). Journal of Magnetic Resonance, 2015, 257: 32–38

[108] Jugniot N, Duttagupta I, Rivot A, et al. An elastase activity reporter for electronic paramagnetic resonance (EPR) and Overhauser-enhanced magnetic resonance imaging (OMRI) as a line-shifting nitroxide. Free Radical Biology & Medicine,

2018, 126: 101–112

[109] Ajoy A, Liu K, Nazaryan R, et al. Orientation-independent room temperature optical ^{13}C hyperpolarization in powdered diamond. Science Advances, 2018, 4(5): eaar5492

[110] Kwiatkowski G, Jähnig F, Steinhauser J, et al. Direct hyperpolarization of micro- and nanodiamonds for bioimaging applications — Considerations on particle size, functionalization and polarization loss. Journal of Magnetic Resonance, 2018, 286: 42–51

[111] Ardenkjaer-Larsen J H, Fridlund B, Gram A, et al. Increase in signal-to-noise ratio of $>10,000$ times in liquid-state NMR. Proceedings of the National Academy of Sciences of the United States of America, 2003, 100(18): 10158–10163

[112] Boele T, Waddington D E J, Gaebel T, et al. Tailored nanodiamonds for hyperpolarized ^{13}C MRI. Physical Review B, 2020, 101(15): 155416

[113] Chen Q, Schwarz I, Jelezko F, et al. Resonance-inclined optical nuclear spin polarization of liquids in diamond structures. Physical Review B, 2016, 93(6): 060408

[114] Rej E, Gaebel T, Boele T, et al. Hyperpolarized nanodiamond with long spin-relaxation times. Nature Communications, 2015, 6(1): 8459–8466

[115] Merkel T J, DeSimone J M. Dodging drug-resistant cancer with diamonds. Science Translational Medicine, 2011, 3(73): 73ps8

[116] Wu Y, Ermakova A, Liu W, et al. Programmable biopolymers for advancing biomedical applications of fluorescent nanodiamonds. Advanced Functional Materials, 2015, 25(42): 6576–6585

[117] Gismondi A, Reina G, Orlanducci S, et al. Nanodiamonds coupled with plant bioactive metabolites: A nanotech approach for cancer therapy. Biomaterials, 2015, 38: 22–35

[118] Zhang X, Wang S, Fu C, et al. PolyPEGylated nanodiamond for intracellular delivery of a chemotherapeutic drug. Polymer Chemistry, 2012, 3(10): 2716–2719

[119] Zwicke G L, Mansoori G A, Jeffery C J. Utilizing the folate receptor for active targeting of cancer nanotherapeutics. Nano Reviews, 2012, 3: 18496

[120] Kranz C, ed. Carbon-Based Nanosensor Technology. 1st ed. Cham, Switzerland: Springer International Publishing, 2019

[121] Neburkova J, Vavra J, Cigler P. Coating nanodiamonds with biocompatible shells for applications in biology and medicine. Current Opinion in Solid State and Materials Science, 2017, 21 (1): 43–53

[122] Smith A H, Robinson E M, Zhang X Q, et al. Triggered release of therapeutic antibodies from nanodiamond complexes. Nanoscale, 2011, 3(7): 2844–2848

[123] Kong X L, Huang L C L, Hsu C M, et al. High-affinity capture of proteins by diamond nanoparticles for mass spectrometric analysis. Analytical Chemistry, 2005, 77(1): 259–265